

Wireless Electric Vehicle charging station.

Abhay Singh¹, UG Scholar, Abhishek Kumar², UG Scholar, Abhishek Panwar³, UG Scholar, Abhishek Sagar⁴, UG Scholar
^{1,2,3,4}Department of Electrical Engineering, IIT Roorkee, Uttarakhand, India E-mail: abhay_s@ee.iitr.ac.in¹, abhishek_k@ee.iitr.ac.in²,
abhishek_p@iitr.ac.in³, abhishek_s@iitr.ac.in⁴.

Abstract--The wireless power transfer technique has been known since the times of Nikola Tesla. Still, in recent years, many successful wireless charging devices have been developed, and wireless charging in the field of electric vehicles has good potential. Our project implements wireless power transfer from AC grid to charge the battery of specified electric vehicle. This report focuses on the fundamentals of WPT and its application for charging electric vehicles. In this the WPT is implemented to charge the battery. The coils are placed at a distance and power transferred to secondary coil placed in the Electric Vehicle. In the primary the AC grid voltage is rectified and then converted to high frequency AC using an inverter. This High frequency AC is then fed to coils to attain higher efficiency power transfer. Different compensation topologies are analysed, and LCC-S topology is used as a compensation circuit. In the secondary side a Buck converter is used to step down the voltage and charge the battery at constant current.

Keywords- wireless power transfer (WPT), high frequency AC, compensation topologies, finite element analysis (FEA)

I. INTRODUCTION

We are moving from using conventional fuel-based vehicles to electric vehicles to reduce pollution and use renewable energy as an alternative to Fossil fuels. To charge an EV, we need charging stations. We have already installed some slow and Fast Charging stations worldwide, but these are wired chargers with different connectors and heavy cables. The wireless power transfer technique has been known since the times of 19th century. Various research in this field is going on and Wireless technology has been developing rapidly in recent years. The transfer efficiency increased to about 90% from several millimetres to hundred millimetres for kilowatt power level.

The storage of electric energy is being a concern over the years. The batteries need to have high energy density, long life cycle and affordable. The energy density of a lithium-ion battery is very poor as compared to combustion engine power vehicle. The batteries used are too heavy and expensive. Also charging of an EV takes a lot of time about several hours based on the power level. By dynamic wireless power transfer system an EV could be powered while driving and it can run non-stop. The battery capacity of EVs can be reduced to 20% with wireless charging which reduce issues like battery cost and long charging time.

The need for wireless charging is that wired charging requires heavy wires and different connectors. Also, chargers are manually connected to EVs. These systems are not user-friendly, and there is always a risk of electric shock (short circuit or electric breakdown) due to poor insulation of wires (due to the high temperature or quality of the charging device). This electric shock can also be fatal. Also, it is quite safe during rainy seasons as there is no wire involved. Wireless charging is more convenient and environment-friendly than wired charging as it provides a better user experience. There is no need to plug-in wires or step out of EVs as the driver of EVs needs to align with the charging pad

and charging starts automatically. Wireless charging of EVs can be helpful in public transportation like buses as it reduces the cost of operation.

II. METHODOLOGY

The main component of a typical wireless EVs charging system is the compensation network and setting up of coil parameters. The main challenge is to deduce the self and mutual inductance of the coil system. Ansys analysis has been used to obtain the inductance values. Along with that we deal with different components of this IPT Model like PFC rectifier, compensation network, battery charging with constant current. PFC rectifier implements a control strategy such that input current is in same phase as input voltage and sinusoidal to reduce harmonic distortion. Along with that control loop will produce constant DC voltage of 400V. Further for IPT to increase the frequency we fed rectified DC voltage to inverter to produce high frequency AC which is fed into resonant network of LCC-S topology. After that the AC voltage induced on secondary coil is converted to DC and fed to the buck converter. The buck converter charges the battery at a constant current of 15A.

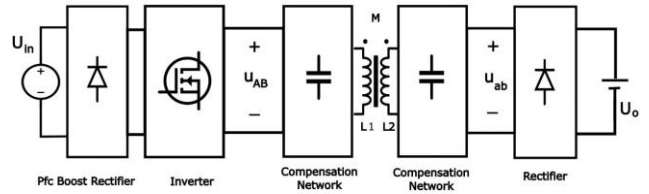


Fig. 1 Typical wireless EV charging system

III. COIL PARAMETER SELECTION

We have used Ansys Maxwell which is a strong finite element analysis (FEA) software program which provides different solvers to calculate the electromagnetic component design. The complete system is divided into different elements according to the mesh (mesh is a three-dimensional grid which defines elements). Behavior of Magnetic field at the interface or edges of the problem region is determined by boundary conditions. The solver which is used is eddy-current solver and in this solver the boundary conditions are determined by box or the air-region and the four end terminals of both the coils touch the boundary.

The relative position between the coils is also a crucial factor which impacts coupling between the coils. From the experiments it is found that as distance between both the coils are increased the coupling coefficient and mutual inductance between the coils decreases.

Many studies have been done to increase the coupling between the coils and one of them is integration of new material in the system, but electrical performance should not

get affected by these materials, the main goal is to improve the coupling between both the coils and decrease (minimize) the leakage flux by directing the flux from the transmitter to the receiver coil. Ferrite bars or plates are mostly used to direct magnetic flux and give magnetic shielding because of high relative permeability of the ferrite and ferrite can reduce the reluctance path and for ferrite hysteresis loss is less as hysteresis loop of Mn-Zn ferrite is narrow.

Due to EVs space constraint we fixed the outer radius of the circular coil at 12.5 cm. A single-lumped-turn winding is used for finite-element simulation to calculate inner radius value and number of turns. For better power transfer efficiency, we must increase coupling coefficient value, so we have varied inner radius of single-lumped-turn winding and plotted coupling coefficient(k) vs inner radius (R_a) shown in Fig 2.3.

Diameter of wire used	3mm
Start radius	60mm
Outer radius	125mm
Radius change	3.5mm
Turns	19
Segments per turn	40
Distance between ferrite core and coil	1.5mm
Ferrite core width	360mm
Ferrite core length	360mm

Table. 1 Coil Specifications

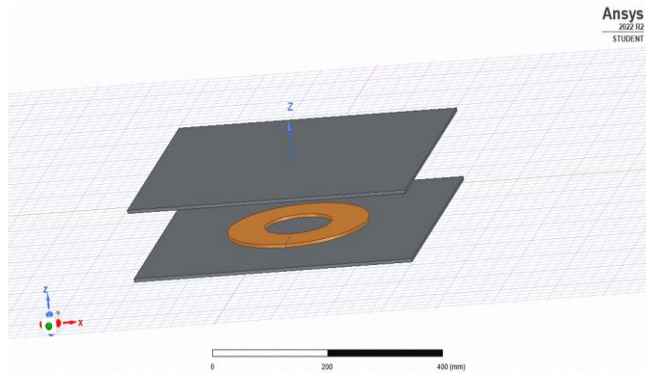


Fig. 2 A single-lumped-turn winding finite-element simulation

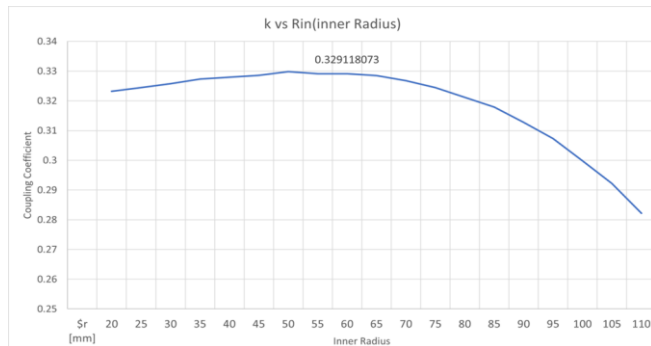


Fig. 3 Coupling Coefficient vs Inner Radius analysis

From the above Fig it is observed that coupling coefficient attains an approximate constant value. So, to reduce wire length the maximum radius with k value of saturated region is taken. The values of coupling coefficient k and value of inner radius comes out to be 0.262 and 6 cm respectively.

IV. RESONANT NETWORK

The inductive power transfer (IPT) occurs between two magnetically coupled inductor coils $L1$ (on primary side) and $L2$ (on secondary side). These coils need to be compensated. According to the type of connection between the coils and their compensation capacitors, there are four basic topologies labelled SS, SP, PP, and PS. The first S/P stands for series/parallel compensation of the primary winding, while the second S/P stands for series/parallel compensation of the secondary winding.

The SS option allows us to select compensatory capacitances solely based on self-inductances, regardless of the load or magnetic coupling while other three the capacitances dependent of coupling variation. Due to its simplicity and desirable load characteristics SS is preferable but when there is no secondary side the equivalent load for the Primary side is nearly zero and infinite current flows which can damage the inductor and for which additional protection is needed.

For multicomponent compensation topologies we have LCC-LCC and LCC-S in which a constant current is induced in secondary side which is also independent of the load variations. The LCC-LCC requires multiple components on secondary side too and for simplifying onboard secondary side the LCC-S topology is considered in this paper.

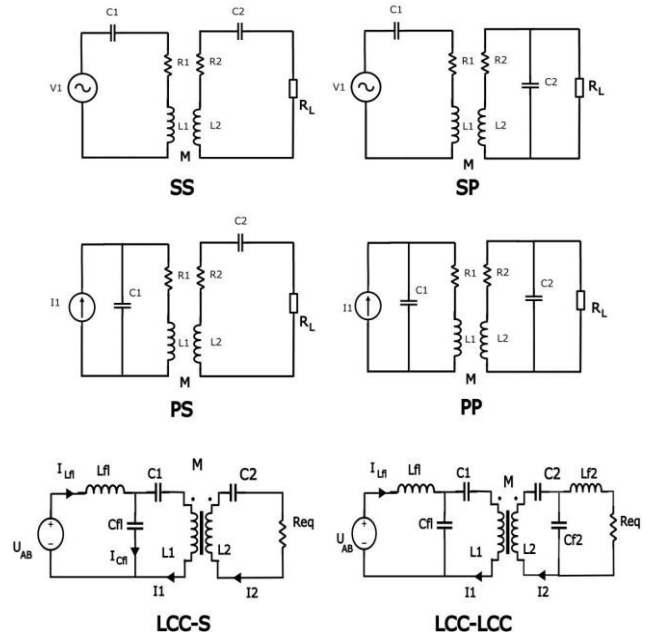


Fig. 4 Different Topologies

A. Determination of Resonant network components values

The industry standards such as SAE J2954 have constrained the operation frequency range which is from 81.38 to 90 KHz. Selecting operating frequency as 85 KHz. Now, the relation between the resonant frequency, coil inductances and

compensation capacitances are given by the equation as given below.

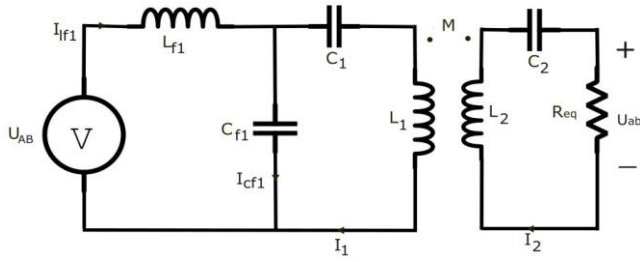


Fig. 5 LCC-S network

v	Description	Design value
L	Primary coil inductance	137.804 μ H
C	Secondary side parallel compensation capacitor	72.82 nF
C	Primary side series compensation capacitor	39.093 nF
L	Primary side compensation inductance	48.138 μ H
L	Secondary coil inductance	137.804 μ H
C	Secondary side series compensation capacitor	25.43 nF
M	Mutual inductance of coil	36.236 μ H
f	Frequency of supply	85 kHz

Table. 2 Compensation network parameter

V. OTHER COMPONENTS

A. Buck Converter

Charging of Battery is done using a current controlled DC-DC Buck converter. Here the duty ratio for constant current charging of battery with buck converter is controlled using a PI controller tuned by auto-tuning method available in the MATLAB. First, a mathematical model

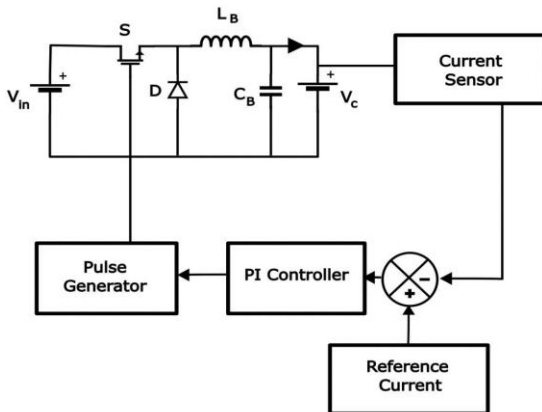


Fig. 6 Closed loop control of Buck converter

of buck converter is designed using state space approach modelling. A separate simulation is done for this component on MATLAB Simulink.

B. Boost PFC Rectifier

The rectifier acts as an intermediate between the AC grid and power electronic devices like DC regulated power supply and supplying high quality power for power electronics devices. Switching devices are readily used for different conversion devices. The introduction of switching devices improves efficiency but create problems like harmonic pollution and low power factor. To eliminate these a new strategy called power factor correction is used. There has been different kind of topology and control strategies has been studied and evaluated to improve the power factor. In this report PFC boost topology has been used to get power factor correction and to reduce total harmonic distortion. A power factor correction regulator is interposed between AC-main and DC load by this way non-linear load acts as resistive load to the AC line. The AC supply from the AC grid is fed to the inverter through a rectifier and a stable 400V DC is supplied to inverter.

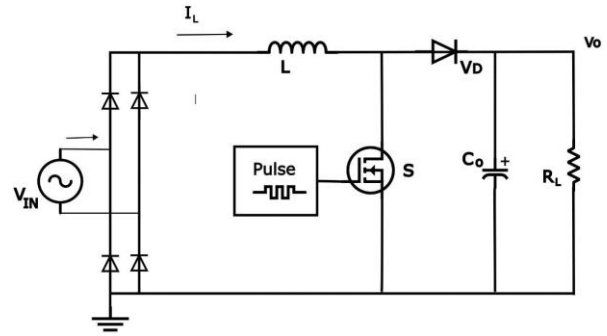


Fig. 7 Boost PFC rectifier

C. Basic Principle of boost PFC Rectifier

The PFC (Power Factor Correction) system comprises a main circuit and a control circuit, with the former consisting of a single-phase bridge rectifier and a DC-DC boost converter. Fig 2.6 represents control circuit of the rectifier. The control circuit includes an outer voltage control loop and an inner current control loop to ensure sinusoidal input

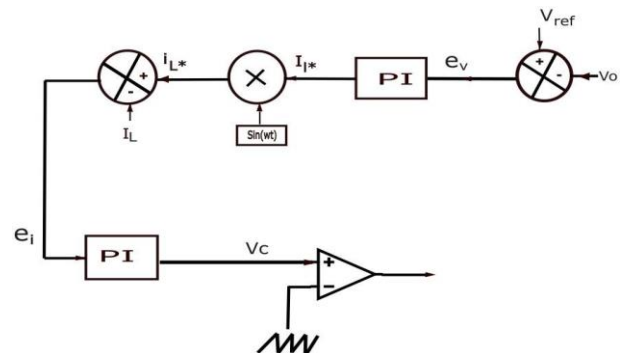


Fig. 8 Closed loop control of PFC rectifier

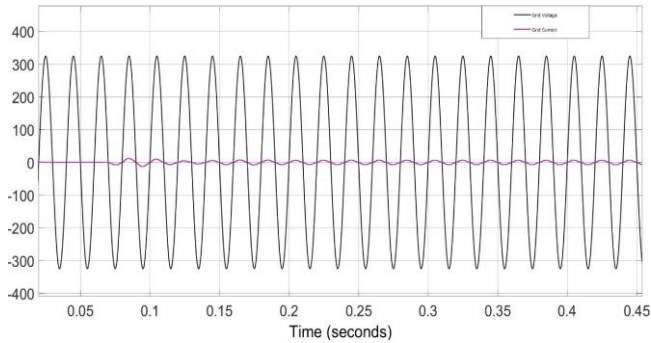
current and maintain DC output voltage. The voltage control output I_L^* is obtained by comparing the output voltage V_o with the reference voltage V_r . To achieve a sinusoidal input current, the inner current control loop multiplies I_L^* with

$\sin(\omega t)$ to obtain a reference signal, which is compared with the input current by the current controller. The PWM generator produces pulses based on the current control output to drive the main switch.

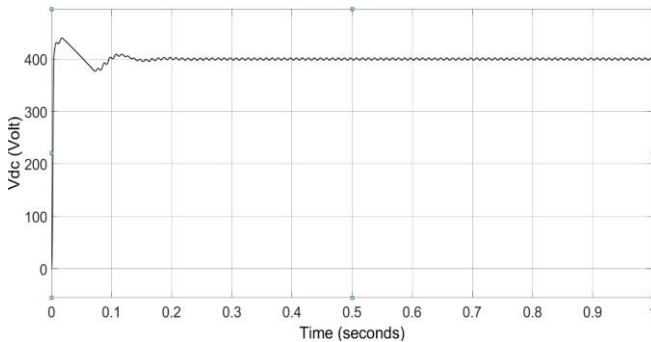
VI. SIMULATIONS AND HARDWARE RESULTS

A. PFC Boost rectifier output

The AC supply fed to the PFC rectifier is 230V, 50Hz. The PFC rectifier produces 400V DC and input current and input voltage are in same phase. This is fed in the inverter to get high frequency (85KHz) AC. Fig 3.2 shows the waveform of input voltage, input current and output voltage.



(a)



(b)

Fig. 9 (a) Grid current and voltage (b) PFC rectifier output voltage

B. Resonant converter output

The gain for the resonant converter is taken as 0.75 and accordingly the value of L_{f1} is calculated. The input of 400V DC is fed to inverter and the output after the secondary side rectifier is 300V DC. Fig 3.3 shows the waveform of output voltage of resonant converter.

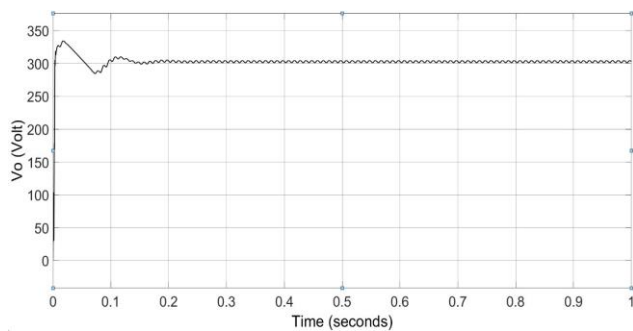
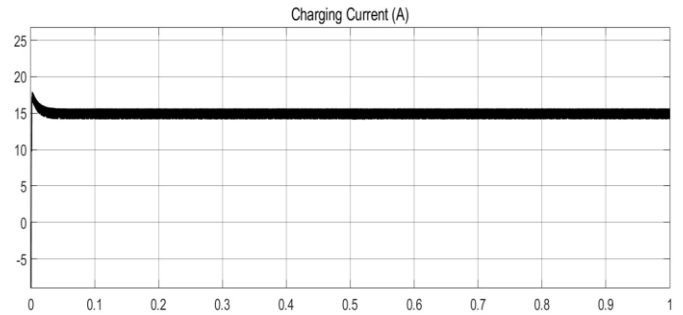


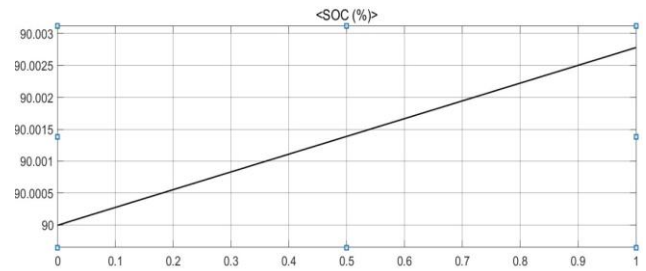
Fig. 10 Resonant network output voltage

C. Battery Charging Output

The battery of capacity 150Ahr, 48V is charged using a buck converter at constant current of 15A. Buck converter is fed by the voltage produced by the resonant converter i.e., 300V DC. The voltage is stepped down to 48V by using a closed loop control strategy with switching frequency of 10KHz. Fig 3.4 shows the state of charge (SOC) of battery, which is linearly increasing with time, waveform of constant current charging.



(a)



(b)

Fig. 11 (a) Battery charging current and (b) SOC%

D. Hardware implementation

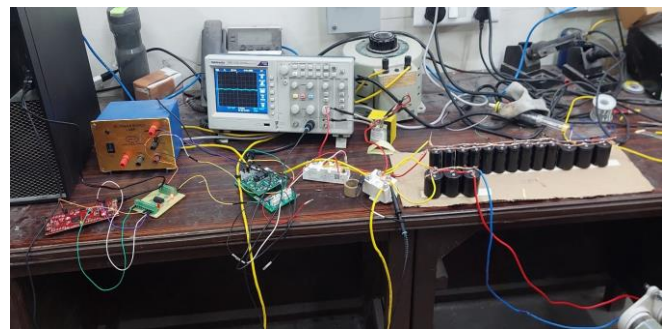


Fig. 12 Hardware Setup with Rectifier and Capacitor Banks

We have designed and implemented a boost converter for power factor correction using a TMS320f28379d microcontroller. The boost converter is used to increase the voltage from 9.64 V to 19.3 V, and a full bridge diode rectifier is used to convert AC voltage to DC before it is fed to the boost circuit. A PWM wave with a frequency of

10KHz and duty cycle of 50% is generated for the boost converter. A level shifter was used to increase the peak voltage of the pulse from 3.3 V to 15 V before it was fed to the gate driver, which runs the IGBT gate. The current is drawn across a load that is connected in parallel to a capacitor bank. This load is likely a resistive load, and the capacitor bank is used to smooth out the voltage across the load. Power factor correction is important because it improves the efficiency of the system and reduces the amount of reactive power that is drawn from the power source [13][14][15].

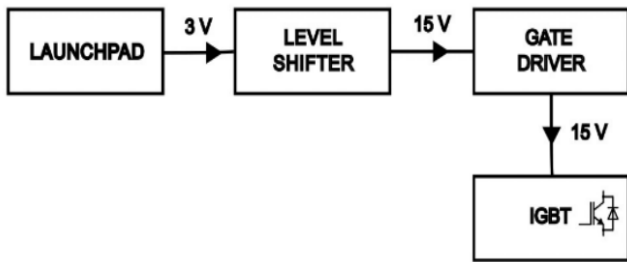


Fig. 13 Schematic diagram of hardware

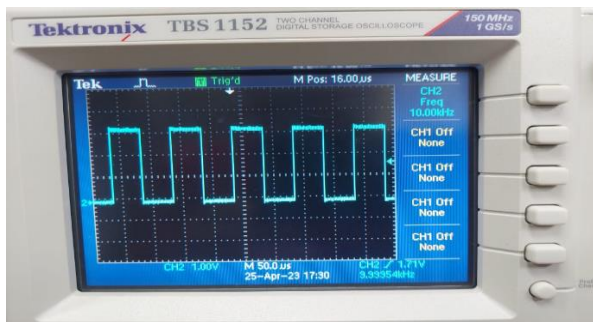


Fig. 14 Pulse generated from microcontroller.

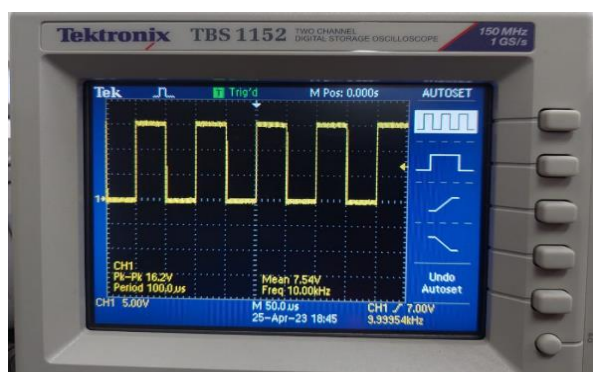


Fig. 15 Pulse after level shifter



Fig. 16 Boosted Voltage output of Boost Converter

VII. CONCLUSION

The report deals with Wireless Charging System for Electric Vehicles. Inductive Power Transfer has been designed for power transfer between two magnetically coupled coils. LCC-S topology is proposed for the circuit model. Coil parameters are evaluated using FEM Analysis using ANSYS Maxwell and resonant network component values are evaluated using gain and resonant conditions.

The electric model is designed on the Simulink taking 230 Volts AC power supply as input and delivering efficient battery charging voltage and current. The model is operated at the resonant frequency of 85Khz to maximize the efficiency of the model. An efficiency of 85% is achieved for a 924 Watts input power into the Li-ion battery. A comparison between different types of batteries has been made by analysing the output power and their advantages over another.

The battery capacity of EVs can be reduced to 20% with wireless charging which reduces issues like battery cost and long charging time. The wireless charging revolution can be made by reducing the overall cost of charging, enabling the people to switch to EVs easily and happily.

VIII. ACKNOWLEDGMENT

We express our gratitude towards the Electrical Engineering Department of IIT Roorkee for giving us the opportunity to deal with a new under the course project named B. Tech Project and helping us improve as undergraduate students.

We would like to thank Prof Premalata Jena and Siba Kumar Patro, express our sincere gratitude for their regular guidance throughout the duration of the project and the trust they put in our group and helped in improving ourselves and the project.

IX. REFERENCES

- [1] J. Deng et al., "Frequency and Parameter Combined Tuning Method of LCC-LCC Compensated Resonant Converter With Wide Coupling Variation for EV Wireless Charger," in IEEE Journal of Emerging and Selected Topics in Power Electronics, vol. 10, no. 1, pp. 956-968
- [2] M. A. Al Mamun, M. Istiak, K. A. Al Mamun and S. A. Rukaia, "Design and Implementation of A Wireless Charging System for Electric Vehicles," 2020 IEEE Region 10 Symposium (TENSYP), 2020.
- [3] S. Bhattacharya and Y. K. Tan, "Design of static wireless charging coils for integration into electric vehicle," 2012 IEEE Third International Conference on Sustainable Energy Technologies (ICSET), 2012.
- [4] F. Pellitteri, V. Boscaio, A. O. Di Tommaso, F. Genduso and R. Miceli, "E-bike battery charging: Methods and circuits," 2013 International Conference on Clean Electrical Power (ICCEP), 2013.

- [5] M. Elshaer, C. Bell, A. Hamid and J. Wang, "DC–DC Topology for Interfacing a Wireless Power Transfer System to an On-Board Conductive Charger for Plug-In Electric Vehicles," in *IEEE Transactions on Industry Applications*, vol. 57, no. 6.
- [6] S. Kim, H. Cha and H. -G. Kim, "High-Efficiency Voltage Balancer Having DC–DC Converter Function for EV Charging Station," in *IEEE Journal of Emerging and Selected Topics in Power Electronics*, vol. 9, no. 1.
- [7] F. Turki, R. Wiengarten, V. Reising and A. Kratser, "Impact of the Working Frequency on Wireless Power Transfer Systems," *PCIM Europe 2014*.
- [8] C. S. Matwankar and A. Alam, "Solar Powered Closed-loop Current Controlled DC-DC Buck Converter for Battery Charging Application," *2019 International Conference on Vision Towards Emerging Trends in Communication and Networking (ViTECoN)*, 2019, pp. 1-5.
- [9] A. Ramezani, S. Farhangi, H. Iman-Eini, B. Farhangi, R. Rahimi and G. R. Moradi, "Optimized LCC-Series Compensated Resonant Network for Stationary Wireless EV Chargers," in *IEEE Transactions on Industrial Electronics*, vol. 66, no. 4, pp. 2756-2765.
- [10] K. Mahmud and L. Tao, "Power factor correction by PFC boost topology using average current control method," *2013 IEEE Global High Tech Congress on Electronics*, 2013, pp. 16-20, doi: 10.1109/GHTCE.2013.6767232.
- [11] Ziyong Liu "Design of single-phase 4 boost power factor correction circuit and controller applied in electric vehicle charging system" *2016 Worcester polytechnic institute*.
- [12] Ming Lu, Khai D.T. Ngo , " Systematic Design of Coils in Series–Series Inductive Power Transfer for Power Transferability and Efficiency".
- [13] [SEMIKRON_DataSheet_Board_1_SKYPER_32_R_L6100131.
- [14] Texas Instruments, "TMS320F2837xD Dual-Core Microcontrollers".
- [15] Texas Instruments, "CCS/TMS320F28335: How to use TMS320f28335 for beginner".